

## Sum Frequency Generation Imaging Microscopy of CO on Platinum

Katherine Cimatu and Steven Baldelli\*

Department of Chemistry, University of Houston, Houston, Texas 77204

Received October 6, 2006; E-mail: sbaldelli@uh.edu

Heterogeneous catalytic reactions of small molecules have been widely investigated throughout the years including the adsorption and reaction of carbon monoxide (CO) on metal surfaces,<sup>1</sup> such as single and polycrystalline platinum.<sup>2,3</sup> Most techniques used in surface investigations measure an average response over the probe area and assume that it is representative of the whole sample. However, even well-prepared metal surfaces contain defects from the angstroms (Å) to micrometers (μm) size range, and this often leads to misinterpretation of the data analysis.<sup>4</sup> To probe local heterogeneity, we use sum frequency generation vibrational spectroscopy as an imaging technique to investigate the distribution of CO adsorption on the platinum surface versus the average response to determine the degree of heterogeneity. By only obtaining the surface averaged spectra, the results lead to an incomplete or even erroneous understanding of the surface.

Several methods have been developed that are capable of imaging monolayers on surfaces with varying degrees of spatial, temporal, and chemical resolution.<sup>4</sup> Of note in these respects are PEEM (photo electron emission microscopy), micro-NEXAFS (near edge X-ray absorption fine structure), AFM/STM, and miscellaneous micro-electron and X-ray techniques.<sup>4</sup> Photoelectron spectroscopy (PES) is a very sensitive surface technique that has been used for many decades in the surface science community. Recently, PES has been used in the imaging mode of the PEEM technique.<sup>5</sup> However, these techniques must also be performed in high vacuum systems.

One of the breakthroughs in surface vibrational spectroscopy is sum frequency generation spectroscopy (SFG) which has excellent chemical selectivity and interfacial specificity even at ambient temperature and pressure and on a variety of interfaces.<sup>6</sup>

SFG is a second-order nonlinear process where a signal is generated from molecules in a noncentrosymmetric environment.<sup>7</sup> This process is described by the second-order susceptibility<sup>8</sup>

$$\chi^{(2)} = \chi_R^{(2)} + \chi_{NR}^{(2)} = |\chi_{NR}^{(2)}| e^{i\phi} + \sum_q \frac{A_q}{\omega_{IR} - \omega_q + i\Gamma}$$

The sum frequency generation imaging microscopy (SFGIM) technique provides images of the surface where the contrast is based on the inherent vibrational spectrum of the adsorbed molecules.<sup>9</sup>

For this experiment, a home-built SFG imaging microscope is used to obtain both the vibrational spectrum (average) and images of the monolayer at the same time. The instrument involves the spatial and temporal overlap of a fixed 1064 nm beam and a tunable IR beam that generates the SFG beam at a specific angle and wavelength. The generated SFG signal is imaged onto a CCD camera.<sup>9</sup> SFG imaging experiments were performed in pp polarization for input light fields. Images and spectra were obtained by continuously scanning the infrared frequency at a set scan rate and averaging the SFG signal over a 5 cm<sup>-1</sup> interval. Image acquisition was 5000 shots/image from 2000–2150 cm<sup>-1</sup>. Local spectra were obtained by averaging a 50 × 50 μm<sup>2</sup> area of the whole image for every 5 cm<sup>-1</sup>. Vibrational spectra are acquired by extracting the

intensity and plotting as a function of the infrared frequency using Origin software.<sup>9</sup>

Although the spatial resolution of this microscope is <10 μm, the SFG images are spectrally analyzed by dividing the image into 50 × 50 μm<sup>2</sup> grids, extracting the spectrum (Figure 1F) and normalizing to the highest intensity peak. This process helps to eliminate the variation of the Gaussian laser profile across the surface. Spectra were fitted using a Lorentzian line shape function for analysis of peak amplitude, frequency, width, and phase shift.<sup>8</sup> These values at each region are then mapped back onto the surface and presented in Figure 2.

The platinum surface was prepared by using a standard method of successive polishing down to 0.05 μm alumina–water slurry (Al<sub>2</sub>O<sub>3</sub>) to produce a surface with a mirror finish and flame-annealing in a hydrogen gas (H<sub>2</sub>) + air flame.<sup>10</sup> The sample was transferred to a vacuum-tight SFG cell, evacuated to 1 × 10<sup>-5</sup> Torr and backfilled with CO (g) to a pressure just over 1 atm.<sup>11</sup> After preparation, the sample was aligned in the microscope.

Figure 1 presents the images taken using SFGIM at selected vibrational frequencies. From the spectra, only top-site CO is observed consistent with the previous average studies of CO on polycrystalline platinum surfaces.<sup>12–14</sup> However, SFG images reveal that some local spectra of CO on Pt are quite different from the average spectrum (Figure 1) and leads to the conclusion of a heterogeneous surface. Bright and dark regions are observed on the images as the IR frequency changes, and this is the basis for contrast in the images. The bright regions are due to enhanced SFG intensity (peak) with one vibrational resonance, and the dark regions are approximately zero intensity. Six SFG spectra are extracted from the region indicated by the bar in Figure 1. The peak assignments of low and high CO vibrational frequencies are at 2062 and 2083 cm<sup>-1</sup>, respectively. A variation in peak position is observed from different regions in the images.

Chemical maps of the CO distribution on the surface as well as a histogram of peak positions are presented in Figure 2. The maps illustrate the spatial distribution of the low-frequency and high-frequency species over the image area. The histogram demonstrates the variety of CO peaks present as well as the clustering of values near 2062 and 2083 cm<sup>-1</sup>. Without prior knowledge of two distinct types of CO on the surface, the average SFG spectra could either be fitted with one or two Lorentzian peaks having equally good *R*<sup>2</sup> values (only a 0.007 difference). Fitting with two peaks is, however, the more physically correct choice.

On the basis of these results and those of previous studies, the vibrational spectroscopy of CO is uniquely sensitive to its chemical and physical environment.<sup>15</sup> In Figure 1, the SFG vibrational spectra were fitted for two peaks between 2000 and 2100 cm<sup>-1</sup>. The frequency of the CO vibration is influenced by several factors and these include the following: (1) surface coverage of CO on Pt<sup>16</sup> attributed to (2) dipole–dipole coupling,<sup>17,18</sup> (3) different coordination sites (kinks, steps, and terraces),<sup>15,19</sup> (4) electronic effect, (5) metal properties bonding, (6) electric fields (vibrational Stark shift

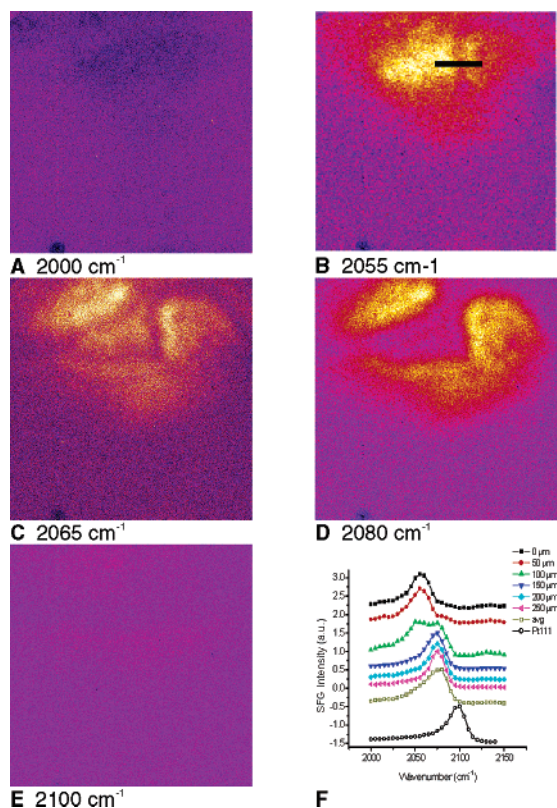


**Figure 1.** (A–E) A false-color, unprocessed SFG image of CO on platinum at  $P_{\text{CO}} = 1$  atm. Images are taken with pp polarization. (F) Spectra are extracted from the images obtained at each wavenumber interval. The bar in image B represents the position where the spectra are extracted, right to left.

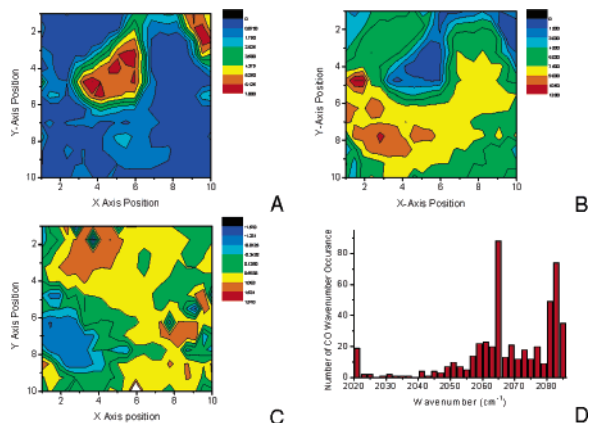


**Figure 2.** SFG image maps of the spatial distribution of CO on a Pt surface (zoom-in on top half of image): (A) the low-frequency peak centered at  $2062 \text{ cm}^{-1}$  and (B) the high-frequency peak centered at  $2083 \text{ cm}^{-1}$  (see Figure 1 for SFG spectra); (C) phase ( $\varphi$ ) map of  $\chi_{\text{NR}}$ ; (D) histogram of the number of occurrences of a CO peak at a specific wavenumber.

effect),<sup>19</sup> and finally, (7) carbon or oxygen co-adsorption from CO dissociation by Boudouart reaction.<sup>20</sup> Most of the peak shifts for

adsorbed CO are usually explained by dipole–dipole coupling in the CO adlayer.<sup>21</sup> Similarly, co-adsorption of carbon or oxygen also affects the SFG spectrum through electronic effects, which are observed as a change in the phase of  $\chi_{\text{NR}}$  (Figure 2C) from the metal.<sup>22–24</sup>

The presence of carbon and oxygen coadsorbed with high-pressure CO on the surface of platinum is consistent with previous results.<sup>20</sup> Adsorbed carbon and oxygen change the SFG spectrum by changing the phase of the metal response and also by reducing the CO coverage, which influences the  $\nu_{\text{CO}}$  by a dipole coupling mechanism.<sup>25</sup>

The results presented here demonstrate the importance of considering that defects and inhomogeneities exist on the surface, which influence the interpretation of SFG data and images. Consequently, by only considering the average signal, many local features of the surface are overlooked and, thus, lead to an inaccurate understanding of the system. The ability to visualize the surface enhances our understanding of surface chemistry.

**Acknowledgment.** We thank Research Corporation for support of this work and John-Glenn Ramon of UH for software development.

## References

- (1) Somorjai, G. A. *Introduction to Surface Chemistry and Catalysis*, 1st ed.; John Wiley and Sons Inc.: New York, 1994.
- (2) Ertl, G. *Science* **1991**, *254*, 1750.
- (3) Somorjai, G. A. *J. Phys. Chem. B* **2000**, *104*, 2969.
- (4) Lipkowsky, J.; Ross, P. N., Eds. *Imaging of Surfaces and Interfaces*; Wiley-VCH: New York, 1999.
- (5) Rotermund, H. H.; Jakubith, S.; von Oetzen, A.; Ertl, G. *Phys. Rev. Lett.* **1991**, *66*, 3083.
- (6) Hunt, J. H.; Guyot-Sionnest, P.; Shen, Y. R. *Chem. Phys. Lett.* **1987**, *133*, 189.
- (7) Huang, J. Y.; Shen, Y. R. In *Laser Spectroscopy and Photochemistry on Metal Surfaces*; Dai, H. L., Ho, W., Eds.; World Scientific: Singapore, 1995.
- (8) Aq term contains the information on IR and Raman transition dipole moments for a  $q$ th vibrational mode of the molecules. Then, the denominator contains the IR ( $\omega_{\text{IR}}$ ) vibrational frequency,  $q$ th ( $\omega_{\text{q}}$ ) resonant vibrational frequency, line width ( $\Gamma$ ), and phase ( $\phi$ ).
- (9) Cimatu, K. C.; Baldelli, S. *J. Phys. Chem. B* **2006**, *110*, 1807.
- (10) Clavilier, J.; Faure, R.; Guinet, G.; Durand, R. *J. Electroanal. Chem.* **1980**, *107*, 205.
- (11) Baldelli, S.; Eppler, A. S.; Anderson, E.; Shen, Y. R.; Somorjai, G. A. *J. Chem. Phys.* **2000**, *113*, 5432.
- (12) Villegas, I.; Weaver, M. J. *J. Am. Chem. Soc.* **1996**, *118*, 458.
- (13) Sheppard, N.; Nguyen, T. T. In *Advances in Infrared and Raman Spectroscopy*; Clark, R. J. H., Hester, R. E., Eds.; Heyden & Sons: Philadelphia, PA, 1978; Vol. 5, p 67.
- (14) Hollins, P.; Pritchard, J. *Prog. Surf. Sci.* **1985**, *19*, 275.
- (15) Iwasita, T.; Nart, F. C. *Prog. Surf. Sci.* **1997**, *55*, 271.
- (16) Yau, S. L.; Gao, X.; Chang, S. C.; Schardt, B. C.; Weaver, M. J. *J. Am. Chem. Soc.* **1991**, *113*, 6049.
- (17) Lambert, D. K. *J. Chem. Phys.* **1988**, *89*, 3847.
- (18) Crossley, A.; King, D. A. *Surf. Sci.* **1977**, *68*, 528.
- (19) Lambert, D. K. *Electrochim. Acta* **1996**, *41*, 623.
- (20) McCrea, K. R.; Parker, J. S.; Somorjai, G. A. *J. Phys. Chem. B* **2002**, *106*, 10854.
- (21) Shigeishi, R. A.; King, D. A. *Surf. Sci.* **1976**, *58*, 379.
- (22) Grubb, S. G.; DeSantolo, A. M.; Hall, R. B. *J. Phys. Chem.* **1988**, *92*, 1419.
- (23) Tom, H. K.; Mate, C. M.; Zhu, X. D.; Crowell, J. E.; Heinz, T. F.; Somorjai, G. A.; Shen, Y. R. *Phys. Rev. Lett.* **1984**, *52*, 348.
- (24) Li, C. M.; Ying, Z. C.; Dai, H. L. *J. Chem. Phys.* **1994**, *101*, 7058.
- (25) Miners, J. H.; Cerasari, S.; Efstathiou, M.; Kim, M.; Woodruff, D. P. *J. Chem. Phys.* **2002**, *117*, 885.

JA067063N